Eighteenth Symposium (International) on Combustion The Combustion Institute, 1981

MECHANISMS OF NO_x FORMATION AND CONTROL: ALTERNATIVE AND PETROLEUM-DERIVED LIQUID FUELS

G. C. ENGLAND,* M. P. HEAP, D. W. PERSHING, R. K. NIHART

Energy and Environmental Research Corporation, 8001 Irvine Boulevard, Santa Ana, California 92705

AND

G. B. MARTIN

U. S. Environmental Protection Agency, Industrial Environmental Research Laboratory, Research Triangle Park, North Carolina 27711

Petroleum-, coal- and shale-derived liquid fuels were burned in a downfired tunnel furnace to assess the impact of fuel properties on the formation and control of NO_x emissions. A nitrogen-free oxidant mixture (Ar, CO_2, O_2) was used to isolate fuel NO_x formation. Under excess air conditions fuel NO_x correlated well with total fuel nitrogen content for both the petroleum and alternate fuels. Under staged combustion conditions the influence of fuel nitrogen content was much less pronounced but equally highly correlated except in the case of a coal-derived liquid.

Exhaust NO_x emissions were found to be directly related to the amount of oxidizable nitrogen species leaving the first stage. NO, HCN and NH_3 concentrations were measured in the fuel-rich zone of the staged combustor as a function of stoichiometry for seven liquid fuels and one CH_4/NH_3 mixture. Similar characteristics were observed for all liquid fuels. As the first stage stoichiometry (SR_1) was reduced, NO concentrations at the first stage exit decreased, but below $SR_1 = 0.8$ HCN and NH_3 concentrations increased. Thus, the total fixed nitrogen (TFN = NO + HCN + NH_3) concentration passed through a minimum. Experimental data also indicated that increasing the temperature of the fuel-rich zone decreased TFN concentration which resulted in reduced exhaust NO_x emissions.

Introduction

Increased coal utilization provides a partial solution to current energy problems; however, the need for a balanced fuel economy and realities of retrofit capability necessitate that in the future many industrial users will be required to burn heavy liquid fuels, both petroleum- and coal- or shale-derived. Since these fuels, particularly the alternativeliquids, have relatively high fuel nitrogen contents, there is potential for increased nitrogen oxides (NO_x) emissions unless preventative measures are taken.[1,2]

Staged combustion has proved to be an effective NO_x control technique for residual oil-fired systems.[2,3,4,5,6] However, optimization has proven to be difficult because of a limited understanding of the controlling mechanisms and the trade-off with smoke emissions. This paper summarizes a series of experimental investigations carried out at atmospheric pressure to define the influence of fuel properties and combustor design parameters on NO_x formation. Twenty-six petroleum-, shale- and coal-derived liquid fuels were burned in a refractory-lined tunnel furnace. In-flame measurements were made to quantify the influence of temperature and stoichiometry on the fate of fuel nitrogen species. The ultimate objective of the study was to provide design criteria for full-scale low emission oil burners suitable for a wide range of fuels. The approach was to divide the overall heat release process into a series of zones: 1) a fuel vaporization region; 2) a fuel-rich hold-up zone; 3) a second stage air addition zone; and 4) a burnout zone. The results presented in this paper are mainly concerned with the optimization of the fuel-rich hold-up zone.

*Author to whom correspondence should be directed.

Experimental Systems

Tunnel Furnaces

The fuel comparison tests in this study were done in a downfired, tunnel furnace which has been described in detail previously.[7] The vertical combustion chamber was 2.1 m long and 20 cm in inside diameter. The overall outer diameter was approximately 81 cm and the walls consisted of insulating and high temperature castable refractories. All airstreams were metered with precision rotameters and the artificial atmospheres were supplied from high pressure cylinders.

The staged combustion tests were conducted in a separate but similar tunnel furnace illustrated in Fig. 1. In this system the vertical combustion chamber was 2.3 m long and 15.2 cm in inside diameter. The walls contained slots which allowed insertion of stainless steel cooling coils, thus, the temperature profile within the furnace could be significantly changed by varying the location and number of these coils. The slots were also used for inserting a refractory choke/secondary air injection system. A 5 cm inside diameter choke was used to prevent recirculation of second stage air into the first stage. The secondary air injector was a 10.2 cm diameter stainless steel ring with 24 6.3 mm diameter holes drilled parallel to the axis of the furnace. The injector was designed to provide gradual mixing of the secondary air with the primary combustion products. The velocity ratio of the secondary air to the incoming combustion products was approximately 2-to-1 at a first-stage stoichiometry of 0.8. In some tests a second refractory choke was also inserted near the top of the furnace to shield the initial fuel vaporization zone from cooling coils in the first stage. This "radiation choke" made it possible to vary temperatures in the fuel-rich hold-up zone without influencing the rate of droplet vaporization and initial combustion.

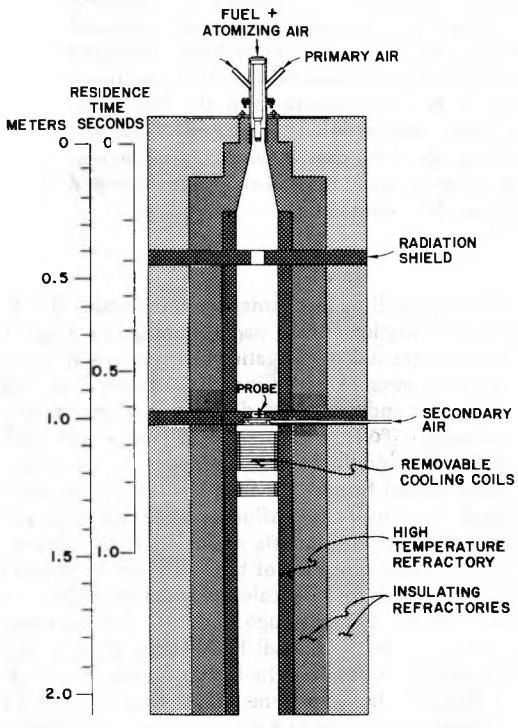

FIG. 1. Furnace configuration showing approximate residence time for $SR_1 = 0.78$.

The full-load firing rate in all experiments (both furnaces) was 0.53 cc/sec. In both systems the fuel injector consisted of a 19 mm diameter stainless steel tube containing an atomizing air supply tube, fuel supply tube, a cartridge heater for final oil temperature control, and a chromel/alumel thermocouple for accurate measurement of oil temperature. A commercial, ultrasonic oil atomizer was used because it provided excellent atomization of the heavy fuel oils at relatively low flow rates even though the atomizer is designed for lighter oils. The spray from this atomizer has been characterized in a separate study using a laser diffraction drop size analyzer and produces a very narrow distribution of drop sizes centered at 20 μm under the operating condition of these experiments.

Analytical System

Exhaust concentrations were monitored continuously using a chemiluminescent analyzer for NO and NO_x, an NDIR analyzer for CO and CO_2, a paramagnetic analyzer for O_2, and an FID analyzer for total hydrocarbons (THC). The flue gas was withdrawn from the exhaust stack through a water-cooled, stainless steel probe using a stainless steel/Teflon sampling pump. Sample conditioning prior to the instrumentation consisted of an ice bath water condenser and glass wool and Teflon fiber filters. All sample lines were 6.3 mm Teflon and all fittings Type 316 stainless steel.

In-flame temperature measurements were made using a standard 19 mm diameter suction pyrometer containing a platinum-platinum/rhodium thermocouple. In-flame gas samples were withdrawn with a long, stainless steel water-quench probe. HCN and NH_3 were absorbed in a series of impingers and concentrations determined using specific ion electrodes. Sulfide ion interference was minimized by the addition of lead carbonate.[8]

Fuels

An independent laboratory determined the characteristics of the liquid fuels used in this study which are given in Table I.

Fuel Effects-Excess Air

Figure 2 is a composite plot of total and fuel NO_x emissions for all of the fuels tested at 5 percent excess O_2, 405°K air preheat and 0.53 cc/sec firing rate. All data were obtained with the ultrasonic nozzle and an air atomization pressure of 103 kPa (gage). Fuel viscosity was maintained at 12 ± 1.5 cs by appropriate selection of fuel temperature. Total NO_x refers to emissions produced with air as the oxidant. Fuel NO_x is defined as the emissions measured when molecular nitrogen was excluded and the fuel burned in an atmosphere composed of argon, carbon dioxide and oxygen.[7] Results obtained with petroleum-derived fuels are presented in Figure 2a. Both total and fuel NO_x emissions increase with increasing fuel nitrogen content. Distillate oils doped with pyridine and thiophene (slashed symbols) correlate well with the actual heavy petroleum liquids under the conditions of these tests (fine oil atomization, rapid mixing burner). The difference between total and fuel NO_x data is defined to be thermal NO_x and is approximately constant for all the heavy residual oils. However, thermal NO_x produced from distillate oils is consistently higher than that produced from residual oils.

A comparison of total and fuel NO_x produced with alternative and petroleum-derived fuels is presented in Figure 2b. In general, alternative fuels have higher nitrogen contents than petroleum-derived fuels and, therefore, produce higher fuel NO_x emissions. With few exceptions, fuel NO_x emissions from both alternative and petroleum-derived fuels appear to correlate well on the basis of fuel nitrogen content. Total NO_x emissions from alternative fuels (dashed line) are higher than from pure petroleum-derived fuels, suggesting a greater production of thermal NO_x. This may be because the alternative fuels contain significantly larger fractions of light hydrocarbons which cause higher peak flame temperatures since more fuel is burned prior to vitiation of the combustion air with recirculated combustion products, or because the relatively high vaporization rates produce higher local combustion intensities.

Staged Combustion

First Stage Stoichiometry

During fuel-rich combustion the original fuel nitrogen species are ultimately converted to N_2,

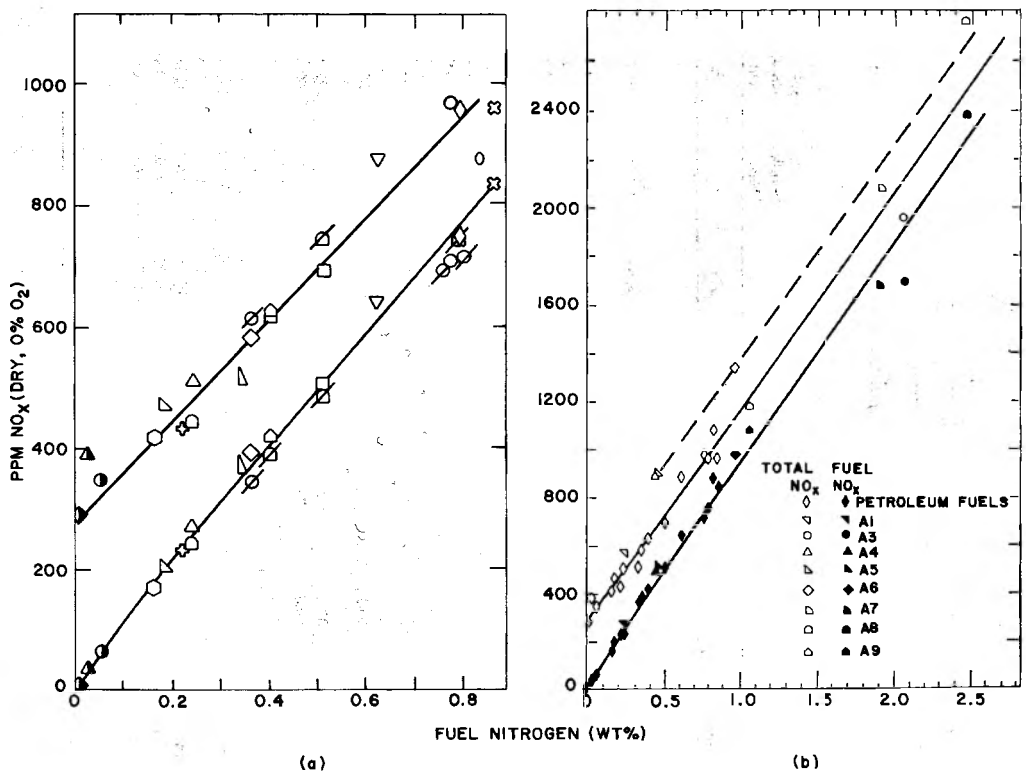

FIG. 2. Total and fuel NO_x produced by (a) petroleum oils (/ denotes doped distillate or residual oils) and (b) all liquid fuels.

TABLE I
Detailed fuel analyses

	D1	D2	D3	R1	R2	R3	R4	R5	R6	R7	R8	R9	R10
	Alaskan Diesel	W. Texas Diesel	California No. 2 Oil	East Coast	Middle East	**Low Sulfur** No. 6 Oil	**Indo/** Malaysian	**Venezuelan Desulfurized**	Pennsylvania (Amarada Hess)	Gulf Coast	Venezuelan	Alaskan	California
Symbol	◆	▲	◑	⬡	◺	✚	△	⌂	◺	◇	⌂	□	▽
Ultimate Analysis:													
Carbon, %	86.99	88.09	86.8	86.54	86.78	86.57	86.53	85.92	84.82	84.62	85.24	86.04	85.75
Hydrogen, %	12.07	9.76	12.52	12.31	11.95	12.52	11.93	12.05	11.21	10.77	10.96	11.18	11.83
Nitrogen, %	0.008	0.026	0.053	0.16	0.18	0.22	0.24	0.24	0.34	0.36	0.40	0.51	0.62
Sulfur, %	0.31	1.88	0.27	0.36	0.67	0.21	0.22	0.93	2.26	2.44	2.22	1.63	1.05
Ash, %	<.001	<.001	<.001	0.023	0.012	0.02	0.036	0.033	0.067	0.027	0.081	0.034	0.038
Oxygen, %	0.62	0.24	0.36	0.61	0.41	0.46	1.04	0.83	1.3	1.78	1.10	0.61	0.71
Conradson Carbon Residue, %				**2.1**	**6.0**	**4.4**	**3.98**	**5.1**	12.4	14.8	6.8	12.9	
Asphaltene, %				0.34	3.24	0.94	0.74	**2.59**	4.04	7.02	8.4	5.6	
Flash Point, °F				205	350	325	210	176	275	155	210	215	
Pour Point, °F				50	48	105	61	48	66	40	58	38	
API Gravity at 60°F	33.1	18.3	32.6	24.9	19.8	25.1	21.8	23.3	15.4	13.2	14.1	15.6	19.5
Viscosity, SSU, at 140°F	33.0	32.0	30.8	131.2	490	222.4	199	113.2	1049	835	742	1,071	246.1
at 210°F	29.5	28.8	29.5	45	131.8	69.6	65	50.5	240	181	196.7	194	70.00
Heat of Combustion:													
Gross Btu/lb			19,330	19,260	19,070	19,110	19,070	18,400	18,520	18,240	18,240	18,470	
Net Btu/lb				18,140	17,980	17,970	17,980	17,300	17,500	17,260	17,400	17,580	
Calcium, ppm				**7.1**	**1.2**	**9.52**	**14**	**8.7**	9.2	4.4	9.1	6.9	
Iron, ppm				**16**	**2.6**	**123.6**	**16**	**6.5**	13.2	19	11	24	
Maganese, ppm				**0.09**	**0.02**	**0.46**	**0.13**	**0.09**	0.10	0.13	0.09	0.06	
Magnesium, ppm				**3.7**	**0.08**	**2.23**	**3.6**	**3.6**	3.3	0.4	3.8	1.4	
Nickel, ppm				6.7	13	14.10	19		32.7	29	52	50	
Sodium, ppm				37	0.98	3.74	15		64.5	3.6	32	37	
Vanadium, ppm				14	25	3.11	101		81.5	45	226	67	

TABLE I
(continued)

	R11	R12	R13	R14	A1	A2	A3	A4	A5	A6	A7	A8	A9
	California	California	California	California (Kern County)	Shale-Derived DFM	Synthoil	Crude Shale	SRC II Blend	Shale Residual	SRC II	Shale Fraction (520–850°F)	Shale Fraction (+850°F)	SRC II Heavy Distillate
	○	◇	⛒	⬯	◥	■	●	▲	◣	◆	◣	◗	◗
Ultimate Analysis:													
Carbon, %	85.4	85.33	86.66	86.61	86.18	86.30	84.6	89.91	86.71	85.91	85.39	85.92	88.98
Hydrogen, %	11.44	11.23	10.44	10.93	13.00	7.44	11.3	9.27	12.76	8.74	11.53	10.61	7.64
Nitrogen, %	0.77	0.79	0.86	0.83	0.24	1.36	2.08	0.45	0.46	0.96	1.92	2.49	1.03
Sulfur, %	1.63	1.60	0.99	1.16	0.51	0.80	0.63	0.065	0.28	0.30	0.72	0.63	0.39
Ash, %	0.043	0.032	0.20	0.030	0.003	1.56	.026	0.004	0.009	0.04	0.002	0.24	0.058
Oxygen, %	0.71	1.02	0.85	0.44	1.07	2.54	1.36	0.30	0.03	4.08	0.44	0.11	1.90
Conradson Carbon Residue, %	8.72	9.22	15.2	8.3	4.1	23.9	2.9	6.18	0.19	0.51	0.07	9.3	
Asphaltene, %	5.18	5.18	8.62	3.92	0.036	16.55	1.33	4.10	0.083		0.12	4.24	
Flash Point, °F		150	180	225	182	210	250	70	235	173	255	370	265
Pour Point, °F	38	30	42	65	40	80	80	<−72	90	−55	70	95	8
API Gravity at 60°F	15.4	15.1	12.6	12.3	33.1	S=1.14	20.3	10.0	29.0		22.3	12.0	1.3
Viscosity, SSU, at 140°F	854	748.0	720	4630	36.1	10,880	97	40.6	54.3	39	62.9	3050	67.2
at 210°F	129	131.6	200	352	30.7	575	44.1	32.5	37.3		41.8	490	41.3
Heat of Combustion:													
Gross Btu/lb	18,470	18,460	18,230	18,430	19,430	16,480	18,290	17,980	19,350	17,100	18,520	18,000	17,120
Net Btu/lb	17,430	17,440	17,280	17,430	18,240	15,800	17,260	17,130	18,190		17,470	17,030	16,240
Calcium, ppm	21	14	90.6	4.4	0.13	1,670	1.5	0.33	4.20		<0.5	238	
Iron, ppm	73	53	77.2	15	6.3	109	17.9	3.9	<0.5		2.9	86	
Manganese, ppm	0.8	0.1	0.87	0.15	0.06	6.2	0.17	<0.5	<0.5		0.033	1.3	
Magnesium, ppm	5.1	3.8	31.4	1.1		170	5.40	0.17	0.15		0.021	51	
Nickel, ppm	65	82	88.0	68	0.43	2.6	5.00	<0.5	<0.5		<0.5	7.4	
Sodium, ppm	21	2.6	22.3	3.4	0.09	148	11.71	0.31	2.51		<0.1	11	
Vanadium, ppm	44	53	66.2	39	<.1	6.5	<.3	<1.0	<1.0		<0.2	1.1	

HCN, NO or NH_3.[9,10,11] The intent of staged combustion is to minimize the concentration of total fixed nitrogen (NH_3 + NO + HCN = TFN) prior to second stage air addition. Figure 3 presents data obtained from detailed in-flame measurements for a distillate oil (D1-Alaskan diesel), a typical residual oil (R9-Alaskan Bunker C), and an alternate liquid fuel (A9-SRC-II heavy distillate). These measurements were made on the centerline of the furnace at a distance of 103 cm (approximately 630 msec) from the oil nozzle. Detailed radial measurements indicated that the concentration profile was essentially uniform at this location. These in-flame data are reported on a dry, as-measured basis. Second stage air was added at 107 cm subsequent to each in-flame measurement in these experiments to bring overall theoretical air to 116 percent, and exhaust NO_x measurements, $(NO_x)_E$, are also shown (on a dry, 0 percent O_2 basis).

Decreasing the first stage stoichiometric ratio reduced NO concentration leaving the first stage. However, below a stoichiometric ratio of approximately 0.8 significant amounts of hydrocarbons (THC) and HCN were measured. Thus, there exists a minimum in exhaust NO_x concentrations because of a competition between decreased first stage NO and increased oxidizable nitrogen species such as HCN. It should be noted that HCN concentration increased rapidly below SR_1 = 0.75 and that this increase was accompanied by an increase in hydrocarbon content of the partially oxidized combustion products.

Data for the Alaskan diesel oil (Fig. 3a) also show the presence of much smaller but significant concentrations of HCN and NH_3, although this fuel is essentially nitrogen-free. Total conversion of the fuel nitrogen would produce 15 ppm TFN at SR_1 = 0.7. This confirms previous work[10,11,12] which demonstrated that reactions involving hydrocarbon fragments and N_2 or NO can produce HCN.

Total fixed nitrogen measured at the exit of the fuel-rich hold-up zone is presented in Fig. 4 as a function of stoichiometric ratio for the Alaskan diesel oil, three petroleum-derived liquid fuels, three alternate liquid fuels, and methane doped with 0.79 weight percent nitrogen as ammonia. All fuels investigated showed similar trends. TFN reached a minimum concentration at approximately SR_1 = 0.8,

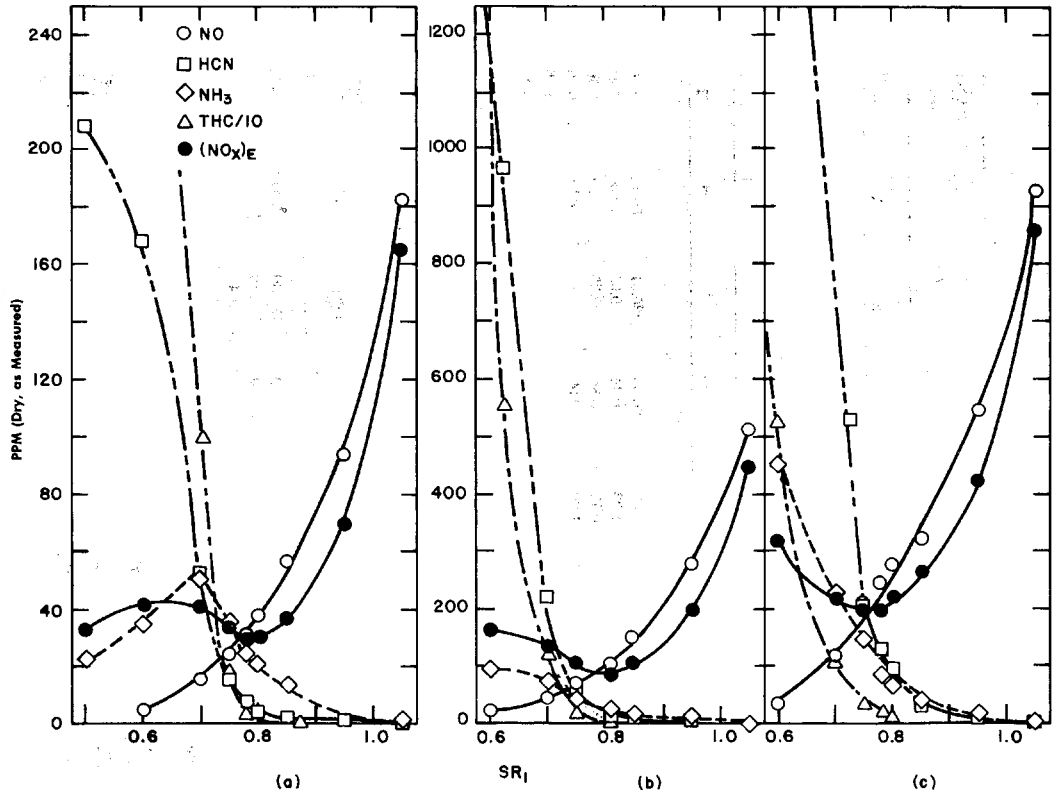

FIG. 3. NO, HCN, and NH_3 production in the fuel-rich hold-up zone for (a) D1-Alaskan diesel oil, (b) R9-Alaskan bunker C oil, and (c) A9-SRC-II heavy distillate oil (3% overall excess oxygen).

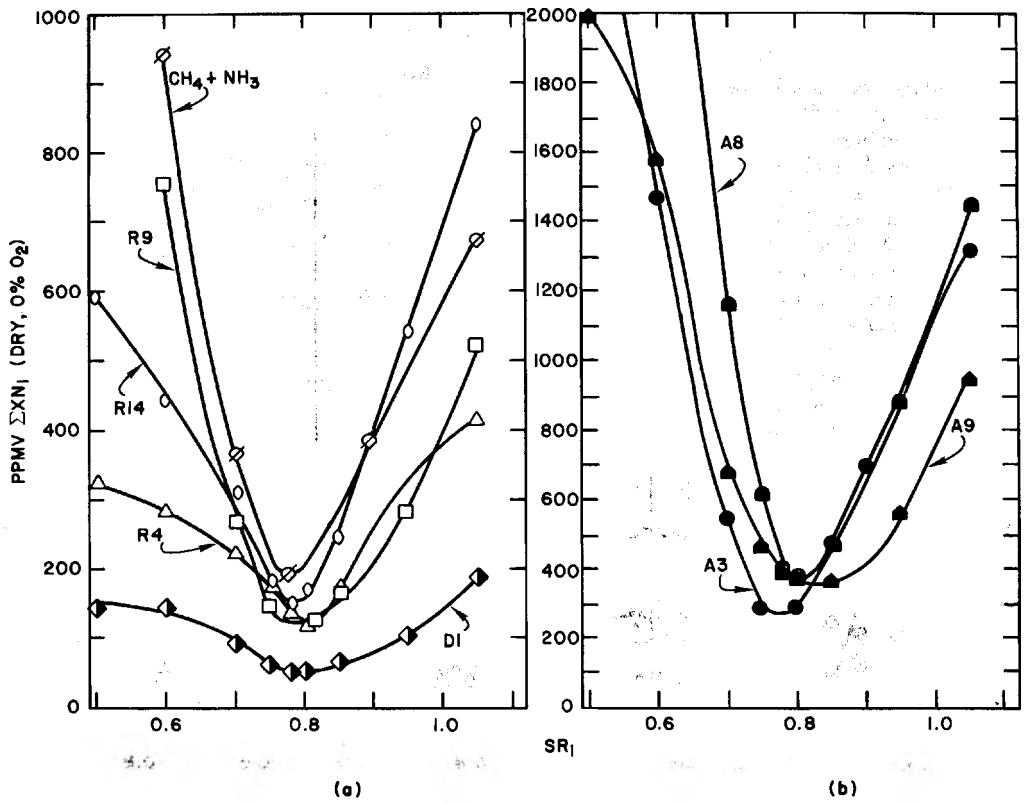

FIG. 4. The effect of fuel type and stoichiometry on the production of TFN (ΣXN_1) for (a) petroleum oils, and (b) alternate fuels.

and then increased significantly as the primary zone became more fuel-rich. The TFN for both the ammonia-doped methane and the fuel oil of similar nitrogen content (R14) showed similar characteristics under fuel-lean conditions. However, below $SR_1 = 0.7$ the heavy oil produced significantly less TFN than the gaseous fuel.

Figure 5 shows the partition of TFN as a function of the first stage stoichiometric ratio. Data for the six liquid fuels and the 0.79 weight percent nitrogen (as NH_3) in methane gas are presented as the percentage of the original fuel nitrogen existing as HCN, NH_3 or NO at the end of the fuel-rich first stage. In each case the missing fuel nitrogen has either been converted to N_2 or still exists in some partially oxidized fuel fragment. All of the liquid fuels exhibited the same general trends:

- Above approximately $SR_1 = 0.8$, NO was the dominant TFN species.
- Below $SR_1 = 0.75$ the major TFN species was HCN and under very fuel-rich conditions HCN usually accounted for more than 50 percent of the initial fuel nitrogen.
- First stage NH_3 levels were always low, generally less than 20 percent of the fuel N. Axial profiles indicated that near $SR_1 = 0.8$, significant amounts of NH_3 were formed early in the rich zone, but decayed rapidly.

Alternative liquid fuels produced TFN distributions very similar to those observed with petroleum-derived liquids. These results are in marked contrast to similar data obtained with pulverized coal[8] which demonstrated that the TFN yield and the preferred species were both strong functions of coal composition.

The fraction of fuel nitrogen converted to HCN was somewhat less for the CH_4/NH_3 mixture (⊘) than for most of the liquid fuels tested (Fig. 5a); however, conversion to NH_3 (Fig. 5b) was higher than the liquids fuels. The light (API = 21.8) Indonesian/Malaysian residual oil (△) produced consistently higher conversion of fuel nitrogen to HCN, NH_3 and NO than the much heavier (API = 12.3) Kern County crude oil (○). Conversely, conversion to HCN and NH_3 for the +850°F shale residuum (■) was higher than for the lighter parent crude shale (●); however, conversion to NO was lower. The exact relationship of

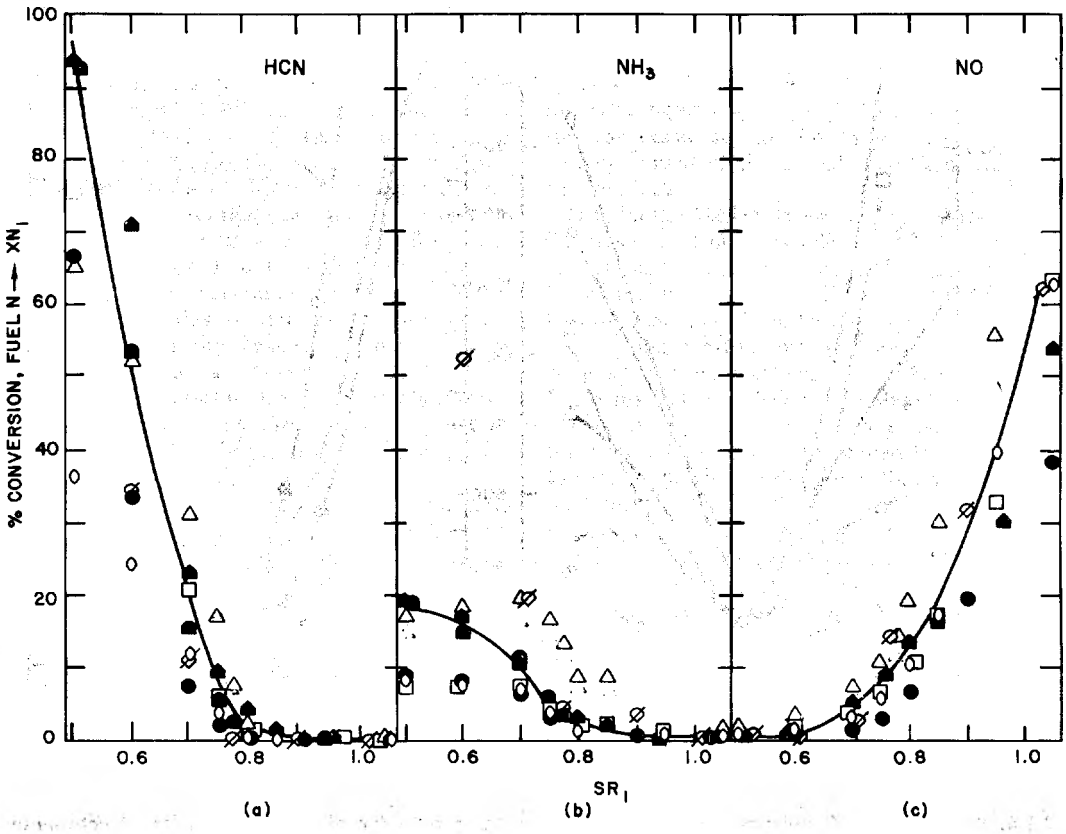

FIG. 5. The conversion of fuel-bound nitrogen to (a) HCN, (b) NH_3, and (c) NO.

simple fuel properties to conversion of fuel nitrogen to intermediate XN species is not apparent at this time.

TFN Conversion in Second Stage

Exhaust NO_x emissions in a staged combustor result from conversion of TFN exiting the first stage and any thermal NO_x production during burnout. Second stage thermal NO_x production is not considered to be significant in this study because changes in heat extraction during burnout had almost no effect on final emissions. Figure 6 shows minimum exhaust NO_x and the associated TFN as a function of total fuel nitrogen content for the seven liquid fuels and the CH_4/NH_3. In general, the minimum exhaust NO_x concentration occurred at $SR_1 = 0.78 \pm 0.02$. Under these optimum staged conditions NO_x emissions (and TFN) correlate well with total fuel nitrogen content, but the slope is significantly less than under excess air conditions (Fig. 2). Only the SRC-II heavy distillate (◆) exhibited unusually high emissions, and this was the direct result of a high TFN yield (Fig. 6b). NO, NH_3 and HCN were all substantially higher for this fuel than with comparable fuels at the minimum stoichiometry (0.78). The increased TFN may be the result of basic chemical bonding differences between the parent coal from which the SRC-II was derived and petroleum liquids.

Figure 7 shows the percent of the TFN exiting the first stage which was converted to NO_x in the second stage (based on NO_x measured in the furnace exhaust). Data for all eight fuels and first stage stoichiometries between 0.5 and 0.8 have been included. As the TFN concentration increased (due to decreasing SR_1), the percentage conversion decreased. This behavior is analogous to that reported previously for poorly mixed excess air diffusion flames.[3,4] The second stage burnout can be considered an excess air flame with a gaseous hydrocarbon fuel. The general conversion decrease may be the result of a competition between N_2 formation reactions which are second order in XN and first order NO formation reactions.

The distillate oil results (◈) in Fig. 7 are substantially below all of the residual petroleum and alternative liquid data and the CH_4/NH_3 results are

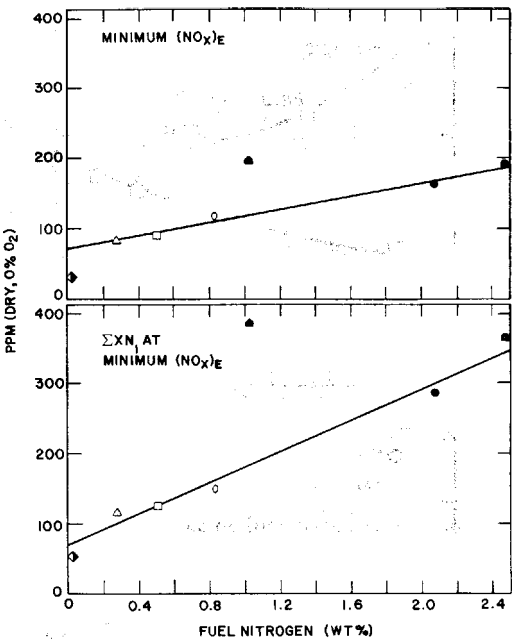

FIG. 6. The effect of fuel-bound nitrogen content on exhaust NO_x and TFN in the primary zone (ΣXN_1) ($SR_1 = 0.78$, 3% overall excess O_2).

slightly high. This suggests that TFN conversion is also dependent on the nitrogen speciation and/or the oxidation of the partial products of combustion at the exit of the fuel-rich zone. At the TFN = 145 ppm point, the first stage exhaust from the distillate oil contained 10,000 ppm hydrocarbons and the dominant TFN species was HCN ($SR_1 = 0.6$). In contrast, the comparable heavy oil points had less than 400 ppm hydrocarbons and NO was the major TFN species ($SR_1 = 0.78$).

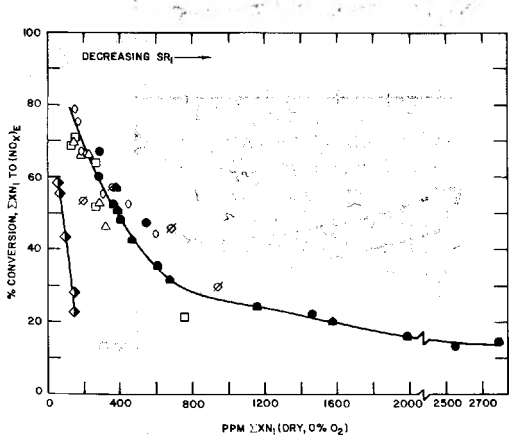

FIG. 7. Conversion of TFN to exhaust NO_x ($0.5 \leq SR_1 \leq 0.8$).

Time-Temperature History

The TFN concentrations shown in Fig. 6 are in excess of equilibrium levels, and Sarofim and coworkers[13] have suggested that increasing the temperature of the primary zone would prove beneficial. The results presented in Figs. 8 and 9 obtained with the shale crude (A3) demonstrate the impact of first stage heat loss on the fate of fuel nitrogen. The hot conditions refer to the furnace without primary zone cooling and with the radiation choke (as shown in Fig. 1). To cool the furnace cooling coils were added prior to the second stage choke and the radiation choke was removed. Figure 8 shows exhaust NO_x and primary zone gas temperature as a function of stoichiometric ratio for the two conditions. Minimum NO_x emissions were reduced for the hot case, and the optimum stoichiometry was shifted toward more fuel-rich conditions.

The axial profiles presented in Fig. 9 provide an explanation for this shift in the minimum emission levels. Heat extraction in the first stage impacts the rate of decay of TFN. Under cold conditions both NO and HCN essentially freeze, whereas without heat extraction the initial rate of decay for all three species is much faster, leading to low TFN concentrations at the exit of the fuel-rich first stage. It should be noted that heat extraction also affects the rate of CO oxidation.

Discussion

NO_x control via staged combustion involves optimizing the first stage of the combustor with respect to (1) thermal environment, and (2) stoichiometry. It appears that heat loss from the first stage should be minimized for liquid fuels because elevated temperatures accelerate the rate of XN species decay toward low equilibrium levels. The data presented in Fig. 8 clearly indicate that an increase in first stage temperature results in a decrease in NO_x emissions.

The optimization of first stage stoichiometry is more complex. Measurements within the fuel-rich first stage show that at the optimum stoichiometry NO, HCN and NH_3 co-exist. TFN exists mainly as HCN and NH_3 for more fuel-rich conditions, and for conditions less fuel-rich than the optimum, NO is the primary fixed nitrogen species. Three factors influence the stoichiometry at which the minimum exhaust NO_x emissions will occur: (1) the amount of TFN species present, (2) the relative conversion efficiencies of the TFN species to NO in the second stage flame, and (3) the influence of other partial combustion products on TFN conversion.

Figure 10a shows the percentage conversion of the first stage TFN for the +850°F shale fraction.

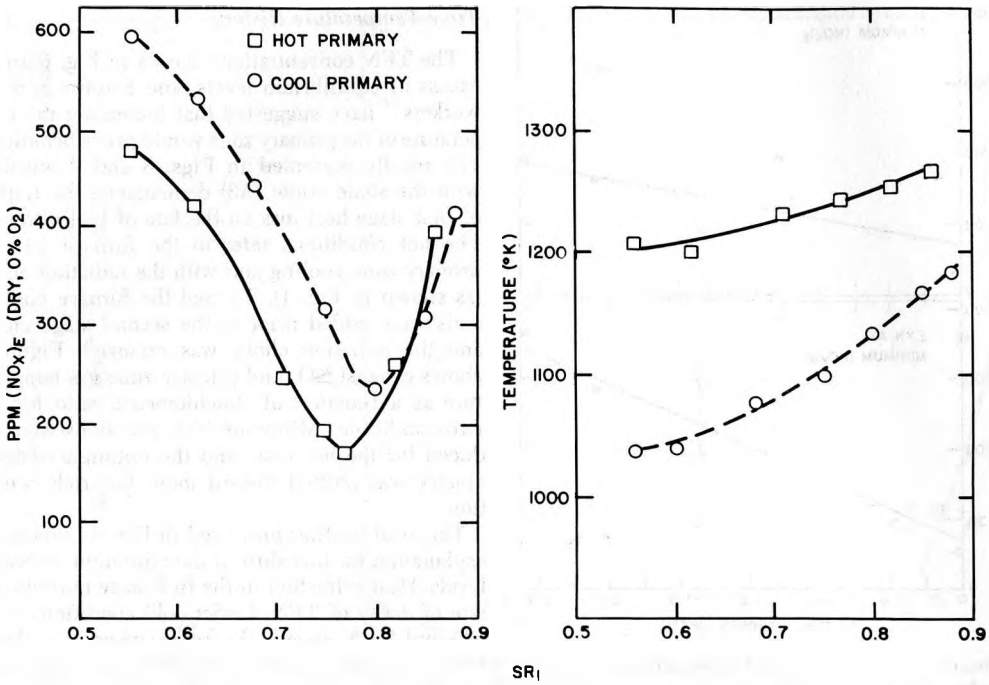

FIG. 8. The influence of fuel-rich hold-up zone temperature profile on exhaust NO_x.

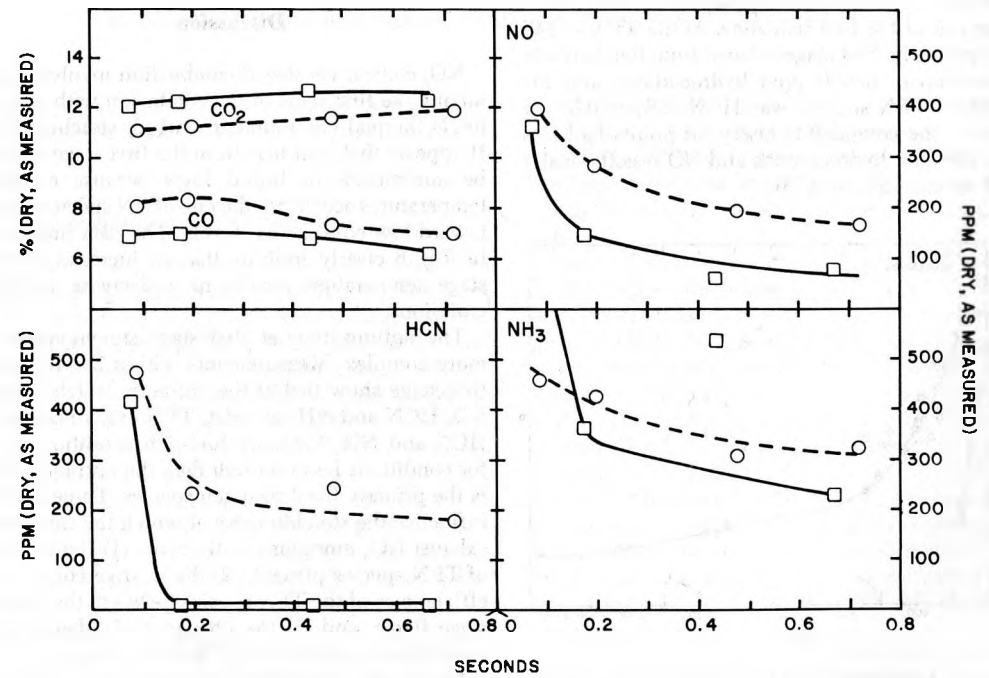

FIG. 9. CO oxidation and decay of XN species for two temperature profiles.

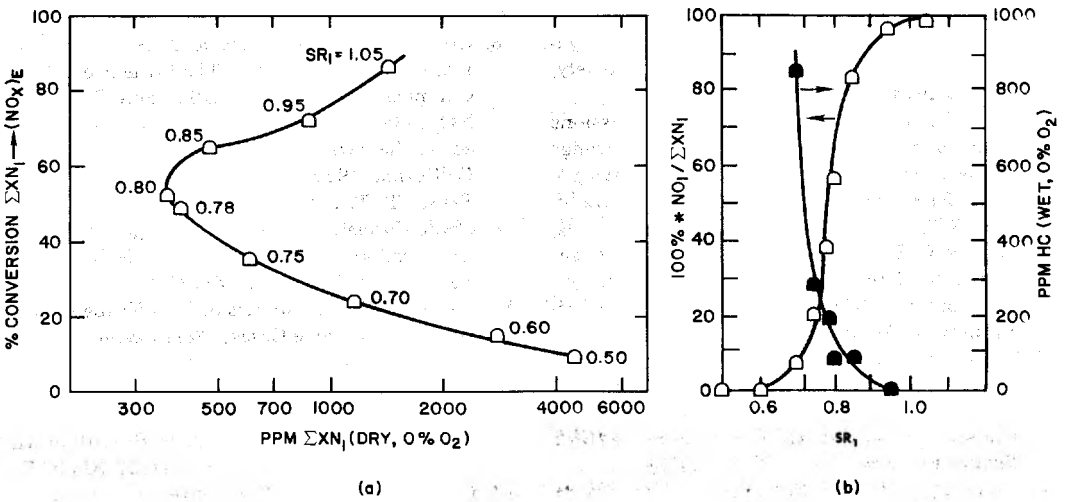

FIG. 10. Influence of first stage exit composition on second stage NO_x formation (A8 – +850°F shale fraction).

As the first stage stoichiometry is progressively reduced from $SR_1 = 1.05$, the TFN decreases (due to decreased first stage NO formation) and the percent conversion also decreases (due to increased second stage combustion). These two effects result in a rapid decrease in exhaust NO_x. Below $SR_1 = 0.8$, the TFN begins to rise dramatically because of HCN and NH_3 formation, but the percent conversion continues to decrease. Thus, in general, there exist two first stage stoichiometries with identical TFN levels (e.g., 1000 ppm) but with vastly different conversion efficiencies (77 percent versus 26 percent) and, hence, different exhaust emissions.

Figure 10b indicates that there are two major differences between the upper and lower percent conversion curves. First, below approximately $SR_1 = 0.8$, the major TFN species shifts from NO to HCN. Second, at first stage stoichiometries less than 0.8, significant amounts of unburned hydrocarbons are carried into the second stage flame. Folsom et al.[14] have shown that in a simple diffusion flame the conversion of HCN and NH_3 to NO and the retention of NO are affected by the hydrocarbon content of the fuel. NH_3 conversion is low when hydrocarbons are absent, and hydrocarbons are necessary for the reduction of NO or HCN to N_2. Thus, staged combustion requires the minimization of TFN, as well as the production of an optimum TFN/fuel mixture for burnout.

Conclusions

Data have been presented showing the impact of fuel properties on NO_x formation from liquid fuels under both excess air and staged conditions. Investigations with a wide range of fuels indicate that:

1. Fuel NO formation from petroleum-, shale- and coal-derived liquid fuels can be correlated by the total fuel nitrogen content under excess air conditions.
2. NO_x control for high nitrogen fuels is most effective when a rich primary zone is held at an optimum stoichiometry to minimize both the TFN concentration and the TFN conversion to NO in the second stage flame. This concentration can be minimized by increasing the temperature of the fuel-rich zone and/or reducing the initial fuel nitrogen content. The second stage conversion decreases with increasing hydrocarbon content.

Acknowledgments

These investigations were carried out under United States Environmental Protection Agency (EPA) Contract 68-02-3125 and the authors gratefully acknowledge the guidance of the Project Officer, W. S. Lanier. The authors also wish to acknowledge the assistance of J. A., Naccarato, J. G., Llanos and J. H. Tomlinson in conducting the experiments, and particularly to W. C. Rovesti of Electric Power Research Institute, J. E. Haebig of Gulf Research and Development Company and L. Lukens of the United States Department of Energy for their help in obtaining several alternative fuels.

REFERENCES

1. MANSOUR, M. N. AND M. GERSTEIN, "Correlation of Fuel Nitrogen Conversion to NO_x During Com-

bustion of Shale Oil Blends in a Utility Boiler," *Symposium on Combustion of Coal and Synthetic Fuels,* American Chemical Society, (March 1978).

2. HEAP, M. P. "Control of Pollutant Emissions from Oil-Fired Package Boilers," *Proceedings of the Stationary Source Combustion Symposium,* EPA-600/2-76-1526, NTIS, Springfield, VA (1976).
3. MARTIN, G. B. AND E. E. BERKAU, "An Investigation of the Conversion of Various Fuel Nitrogen Compounds to NO in Oil Combustion," *AIChE Symposium Series No. 126, 68* (1972).
4. TURNER, D. W., R. L. ANDREWS, AND C. W. SIEGMUND, "Influence of Combustion Modification and Fuel Nitrogen Content on Nitrogen Oxide Emissions from Fuel-Oil Combustion," *AIChE Symposium Series No. 126, 68* (1972).
5. APPLETON, J. P. AND J. B. HEYWOOD, "The Effects of Imperfect Fuel-Air Mixing in a Burner on NO Formation from Nitrogen in the Air and the Fuel," *Fourteenth Symposium (International) on Combustion,* Combustion Institute, Pittsburgh, PA (1973).
6. PERSHING, D. W., G. B. MARTIN, AND E. E. BERKAU, "Influence of Design Variables on the Production of Thermal and Fuel NO from Residual Oil and Coal Combustion," *AIChE Symposium Series No. 148, 71* (1975).
7. PERSHING, D. W., J. E. CICHANOWICZ, G. C. ENGLAND, M. P. HEAP, AND G. B. MARTIN, "The Influence of Fuel Composition and Flame Temperature on the Formation of Thermal and Fuel NO_x in Residual Oil Flames," *Seventeenth Symposium (International) on Combustion,* The Combustion Institute, Pittsburgh, PA (1979).
8. CHEN, S. L., M. P. HEAP, R. K. NIHART, D. W. PERSHING AND D. P. REES, "The Influence of Fuel Composition on the Formation and Control of NO_x in Pulverized Coal Flames," paper presented at the WSS Combustion Institute, Irvine, California (1980).
9. TAKAGI, T., T. TATSUMI AND M. OGASAWARA, "Nitric Oxide Formation from Fuel Nitrogen in Staged Combustion: Roles of HCN and NH_i," *Combustion and Flame, 35, 17* (1979).
10. FENIMORE, C. P., "Studies of Fuel Nitrogen Species in Rich Flame Cases," *Seventeenth Symposium (International) on Combustion,* The Combustion Institute, Pittsburgh, PA (1979).
11. HAYNES, B. S., "Reactions of NH_3 and NO in the Burnt Gases of Fuel-Rich Hydrocarbon-Air Flames," *Combustion and Flame, 28, 81* (1977).
12. GERHOLD, B. W., C. P. FENIMORE AND P. K. DEDERICK, "Two Stage Combustion of Plain and N Doped Oil," *Seventeenth Symposium (International) on Combustion,* The Combustion Institute, Pittsburgh, PA (1979).
13. SAROFIM, A. F., J. H. POHL AND B. R. TAYLOR, "Mechanisms and Kinetics of NO_x Formation: Recent Developments," paper presented at 69th Annual Meeting AIChE, Chicago, November (1976).
14. FOLSOM, B. A., C. W. COURTNEY AND M. P. HEAP, "The Effects of LBG Composition and Combustor Characteristics on Fuel NO_x Formation," paper presented at the ASME Gas Turbine Conference and Exhibit and Solar Energy Conference, San Diego, California (1979).